Itaconate as a Promising Therapy for Neuropathic Pain and Inflammatory Pain

Jinxuan Ren
Zhejiang University School of Medicine Second Affiliated Hospital
Lina Yu
Zhejiang University School of Medicine Second Affiliated Hospital
Jiaqi Lin
Zhejiang University School of Medicine Second Affiliated Hospital
Longfei Ma
Zhejiang University School of Medicine Second Affiliated Hospital
Dave Schwinn Gao
Zhejiang University School of Medicine Second Affiliated Hospital
Na Sun
Zhejiang University School of Medicine Second Affiliated Hospital
Ying Liu
Zhejiang University School of Medicine Second Affiliated Hospital
Lili Fang
Zhejiang University School of Medicine Second Affiliated Hospital
Zhenzhen Cheng
Zhejiang University School of Medicine Second Affiliated Hospital
Kai Sun
Zhejiang University School of Medicine Second Affiliated Hospital
Min Yan (zryanmin@zju.edu.cn)
Zhejiang University School of Medicine Second Affiliated Hospital

Research

Keywords: Dimethyl itaconate (DI), Neuropathic pain, Inflammatory pain, Neuroinflammation, Nrf2, IRG1

Posted Date: April 14th, 2021

DOI: https://doi.org/10.21203/rs.3.rs-404819/v1

Abstract

Background: Chronic pain is a complex experience that often leads to multiple complications. Neuroinflammation in the immune system as well as in the peripheral and central nervous system contributes to the development and persistence of chronic pain. The metabolite itaconate, recently emerged as a regulator of immune cell functions, has features of anti-inflammation and immunomodulation via the activation of Nrf2. However, its effect on chronic pain is unclear.

Methods: Chronic C57BL/6 neuropathic pain and inflammatory pain were induced followed by dimethyl itaconate (DI) treatment, an itaconate derivative. We evaluated the effect of DI on the changes of pain behaviors induced by chronic pain model. The effect of DI on inflammatory cytokine release, glial cells activation, ERK1/2 phosphorylation, inflammatory cell infiltration and Nrf2 expression in the DRGs, spinal cord and hind paw tissues was determined using the histochemistry, RT-PCR and western blot. Microglia was cultured to study the effect of DI on microglial inflammatory response and Nrf2 level.

Results: DI reduced the secretion of inflammatory cytokines in DRGs, spinal cord and hind paw tissues, suppressed the activation of glial cells (like microglia and astrocytes) in spina dorsal horn and infiltration of inflammatory cells in the hind paw tissues, and decreased the phosphorylation of ERK1/2, but boosted Nrf2 levels in the DRGs and spinal dorsal horn. Similarly, administration of DI potently reversed the LPS-induced inflammatory effect in the microglia. Reduction of endogenous itaconate pretreated with irg1 siRNA prevented the expression of Nrf2, which did not exert the analgesic and anti-inflammatory effects in vitro experiment.

Conclusions: Our findings verify for the first time that DI alleviates painful behaviors and suppresses neuroinflammation in neuropathic pain and inflammatory pain models through molecular mechanisms, suggesting that DI elicits sustained chronic pain relief, which will be regarded as a novel therapeutic agent for chronic pain treatment.

Introduction

Chronic pain is a kind of intractable pain, which persists for a long period, even though the initial tissue damage is cured (1, 2). Chronic pain often leads to multiple complications and is a major clinical problem (1). It is characterized by spontaneous pain (such as burning) and evoked pain to noxious (hyperalgesia) or non-noxious (allodynia) stimuli (3) and affects up to 30% of adults worldwide (4) with an annual economic burden of treatment exceeding $600 billion in the USA (4, 5). Due to the complex pathogenesis, currently available treatments have little effect on chronic pain (6). Growing body of evidence demonstrates that the occurrence of neuroinflammation plays an indispensable role in the development and maintenance of chronic pain (7). Its characteristic features involve the activation of glial cells (e.g. microglia and astrocytes), activation and infiltration of leukocytes, and the release of a wide range of inflammatory mediators, such as interleukin (IL)-1β, IL-6, nitric oxide (NO), tumor necrosis factor (TNF)-α both in dorsal root ganglion (DRGs) and spinal cord. Activation of glial cells and immune cells leads to

the development of peripheral and central sensitization (2, 8–11), which is closely associated with the establishment and maintenance of chronic pain (12, 13). Those inflammatory factors, as powerful neuromodulators, can regulate synaptic transmission and plasticity (14) and play an adequate role in inducing hyperalgesia and allodynia in the peripheral nervous system (PNS) and central nervous system (CNS) (3). Given the lack of effective treatments for chronic pain, interventions targeting the neuroinflammatory cascades are considered as promising therapeutic strategies.

Itaconate, an unsaturated dicarboxylic acid, is synthesized by the enzyme immune-responsive gene 1 (IRG1) and participates in the Krebs cycle (15–17). Itaconate has attracted much attention due to its anti-inflammatory (18). As one of the most highly induced metabolites in activated macrophages (19), itaconate can repress pro-inflammatory cytokines production (20) and drive an anti-inflammatory program via the activation of nuclear factor-erythroid 2 p45-related factor 2 (Nrf2) (20, 21) and succinate dehydrogenase (SDH) inhibition (21). Dimethyl itaconate (DI), as a cell-permeable derivative of itaconate, also can effectively activate Nrf2 signaling. DI was found to reduce the expression of pro-inflammatory factors, like IL-1β, IL-6, IL-12 and IL-18 in LPS-stimulated macrophages and ameliorate inflammatory response in mice (20). Due to its anti-inflammatory and immunomodulatory properties, itaconate has recently become a focus of the field of immunometabolism (22). Accumulating studies have shown that itaconate derivatives have therapeutic effects on idiopathic pulmonary fibrosis (23), ischemia-reperfusion injury (24, 25), abdominal aortic aneurysm (26), sepsis (27) and multiple sclerosis (28). However, its effect on neuroinflammation-related chronic pain remains unknown.

In the present study, we confirmed the analgesic effect of itaconate in chronic pain model. We reported for the first time that intraperitoneal (i.p.) administration of DI ameliorated mechanical allodynia and thermal hyperalgesia in neuropathic pain induced by SNL and inflammatory pain induced by Complete Freund's adjuvant (CFA) in mice. In addition, we identified that DI not only suppressed the activation of microglia and astrocytes in the spinal cord, but also inhibited the infiltration of inflammatory cells in the hind paws. Besides, DI blocked the phosphorylation of ERK1/2, enhanced the Nrf2 level and suppressed the production of inflammatory cytokines in DRGs, spinal cord and plantar tissues. In vitro experiments also showed that DI exerted its neuroprotective effect.

Materials And Methods

1. **Animals.**

Male C57BL/6 mice aged 6-8weeks were purchased from Nanjing Institute of Biomedicine and adapted to the study habitat for one week prior to experiment. All animals were subjected to a 12 h:12 h light:dark cycle and fed with free accessed food and water. These mice are randomly divided into groups.

2. Reagents

DI (Cat.no.592498, Sigma, USA), Lipopolysaccharide (LPS) (Cat.no.L2630, Sigma, USA) and CFA (Cat.no.F5881, Sigma, USA) were purchased from Sigma-Aldrich. DI was dissolved in PBS to final concentrations of 10 mg/500 μl and 20 mg/500 μl for in vivo experiment. A volume of 500 μl DI solution was injected into the mice via intraperitoneal route according to previously reported methods (28, 29). DI was dissolved in dimethyl Sulfoxide (DMSO) and diluted to a concentration of 250 μM for in vitro experiment. LPS was diluted in PBS to a concentration of 100 ng/mL.

3. Neuropathic pain model

L4 spinal nerve ligation (SNL) model, as a kind of neuropathic pain model, was induced according to previously reported methods (30). The surgery was done on mice after deeply anesthetized with 1% sodium pentobarbital. In SNL-operated group, isolate the left L4 spinal nerve and tightly ligate it with 6 – 0 silk thread using sterilized operating instruments (Fig. 1, A and B). In sham-operated mice, the left L4 spinal nerve was isolated without ligation. The skin and muscles were finally closed in layers.

4. CFA Model of Inflammatory Pain

Inflammatory pain model was established by CFA (20 μL) that was injected into the plantar surface of the left hind paw (31). The vehicle group received a same volume of saline injection into the same position (Fig. 1C).

5. Behavioral testing

Animals were allowed to habituate to the testing environment for 30min before testing. Mechanical and thermal pain tests were carried out as previously described (32). To test mechanical allodynia, paw withdrawal frequencies (PWF) in response to mechanical stimuli (von Frey filaments) were measured according to the frequency of withdrawal response (the percentage of response) to two calibrated von Frey filaments (0.07 g and 0.4 g, 10 trials of stimulation for each), which were used to stimulate the left hind paw for approximately 1s with at least 5 min interval between two adjacent trials. Paw withdrawal latencies (PWL) to noxious thermal stimulation was tested through the Hargreaves method (IITC Life Science). Withdrawal latency was recorded as the time from the start of irradiation to withdrawal of the tested hind paw. To avoid tissue damage, the cutoff time of heat stimulus was set at 20 sec. The average of three measurements that were repeated at a 15 min interval was regarded as the final PWL for the mouse.

6. Western Blot (WB)

L4 DRGs and L4 spinal cord were harvested from mice day 10 after i.p. injection DI (day 14 after SNL). The L4/5 spinal cord and left hind paw tissues were collected from mice on day 5 after i.p. injection DI in CFA model. Proteins were subjected on 10% SDS-PAGE gel and transferred to PVDF membranes (Millipore, USA). After being incubated with 5% bovine serum albumin, the membranes were infiltrated with primary mouse antibodies against GAPDH (1:1000, Beyotime, China) and GFAP (1:1000, Millipore, USA) and rabbit antibodies against p-ERK1/2 (1:1000, Cell Signaling Technology, USA), ERK1/2 (1:1000,

Cell Signaling Technology, USA) and Nrf2 (1:1000, Abcam, USA; 1:1000, Cell Signaling Technology, USA) at 4° C overnight. The membranes were then incubated with the following secondary antibodies: HRP-anti-rabbit (1:5000, Zhongshan, China) and HRP-anti-mouse (1:5000, Zhongshan, China) at 37° C for 1h. Blots were detected by chemiluminescence (ECL) and exposure to film. The optical densities of protein bands were measured for grey scale densitometric analysis.

7. Real-time quantitative PCR (RT-PCR)

L4 DRGs and L4 spinal cord in SNL model and L4-5 spinal cord and left hind paw tissues in CFA model were collected for RNA extraction. The RNA was isolated using TRIzol reagent (Invitrogen, CA, USA), and the cDNA was synthesized from total RNA (1 μg) using 5×iScript Reaction Mix Reagents (Takara, Japan). Specific primers, including mouse *β-actin*, *tuba1a*, *Il1b*, *tnf*, *Il10* and *irg1* were designed (Table S1). Then the mRNA expression was analyzed by using SYBR Green Premix Ex Taq (Takara, Japan) and QuantStudio 5 real-time RT-PCR instrument (Applied Biosystems, USA). The relative expression levels were presented as -fold changes (ΔΔCt method).

8. Histochemistry

Animals were anesthetized with 1% sodium pentobarbital and slowly perfused with PBS through the ascending aorta, then rapidly perfused with 4% paraformaldehyde. The spinal cord segments (L4) and the left paw tissues were removed and post fixed in 4% paraformaldehyde for 24 h. Subsequently the spinal cord was allowed to equilibrate in 30% sucrose in PBS at 4°C overnight. The spinal cord sections were cut and processed for immunofluorescence. The sections were incubated in PBS containing 4% normal goat serum and 0.3% TritonX-100 at room temperature for 1 h. The samples were incubated with primary antibodies: mouse GFAP (1:200, Millipore, USA) and rabbit IBA-1 (1:200, Wako, USA) at 4°C overnight, washed with PBS for 3 times, followed incubated by donkey anti-rabbit and anti-mouse secondary antibodies conjugated with Alexa Fluor 594 or 488 (1:500; Thermo Fisher Scientific, Waltham, MA, USA) at room temperature for 1 h in the dark. The nuclei were stained by 4',6-diamidino-2-phenylindole (DAPI, Sigma-Aldrich, USA). Images were captured using a fluorescent microscope (DMIRB, Leica, Germany). The left paw tissues were embedded in paraffin and sections (5μm) were stained by hematoxylin and eosin (H&E), and visualized using a light microscope.

9. Cell Culture

BV_2 microglial cell line was provided by Department of Neurosurgery, The Second Affiliated Hospital of Zhejiang University School of Medicine. Cells were grown and routinely maintained in Dulbecco Modified Eagle Medium/F12 (HyClone™) supplemented with 10% fetal bovine serum (FBS, Gibco, USA), 100 U/ml penicillin, and 100 μg/ml streptomycin in a 5% CO_2 atmosphere at 37°C. BV_2 cells were used under passage 20. After 12 h of treatment with DI followed by the stimulation of LPS for 2h, BV_2 were collected and centrifuged at 5000 rpm for 5 min. Cell pellets were then used in follow-up experiment.

10. siRNA transfection of microglia

Cells were planted at 2×10^5 cells per ml in 6-well plates to incubate at 37° C in a CO_2 incubator until the cells are 60–80% confluent. SiRNA was dissolved in RNase-free water at 10 μM as a stock solution. Then, Irg1 siRNA (sc-146287, Santa Cruz Biotechnology, USA) and control siRNA (sc-37007, Santa Cruz Biotechnology, USA) were separately mixed with the transfection reagent (sc-29528, Santa Cruz Biotechnology, USA) to incubate the cells 5–7 hours at 37° C in a CO_2 incubator. Remove the transfection mixture and replace with 1x normal growth medium. Incubate the cells for an additional 18–24 hours.

11. Statistical Analyses.

All data were expressed as mean ± SEM. Two-way repeated-measures ANOVA followed by Tukey's post-hoc test was used for analysis of behavioral data. One-way ANOVA was used for the statistical analyses in other tests. A *P* value of less than 0.05 was considered statistically significant.

Results

1. DI alleviated neuropathic pain after SNL.

The mouse SNL model mimics neuropathic pain induced by nerve injury in the clinical setting (33). In this model, neuropathic pain symptoms such as mechanical allodynia and heat hyperalgesia sustained for many weeks (34). To assess the effect of DI on behavioral signs of neuropathic pain, we continuously administered DI (10 mg or 20 mg) once daily by i.p. injection from day 4 till day 32 after SNL. PWF and PWL was evaluated before surgery (baseline), and on day 1, 3, 5, 7, 11, 18, 25 and 32 day after SNL (Figure 2A). We found that both doses of DI produced an increasing inhibition of SNL-induced mechanical allodynia and thermal hyperalgesia starting from 1 day after injection (Figure 2, B-D). Notably, this antinociceptive effect remained during the 4 weeks period of DI treatment without signs of tolerance. There were no differences in among groups in either mechanical or heat thresholds on the contralateral side of SNL mice (Figure S1, A-C).

2. *Effects of pretreatment of DI on SNL-induced neuropathic Pain Behavior.*

We next examined whether DI pretreatment prevents neuropathic pain. As shown in Figure 3A, two different doses of DI were injected i.p. once daily for consecutive 3 days before and after SNL model. Only the higher dose of DI (20 mg) reversed mechanical allodynia and thermal hyperalgesia during the administration. However, the analgesic effect of 20 mg DI gradually vanished once DI administration was ceased (Figure 3, B-D). Interestingly, the recovery of daily DI supply on day 7 to day 10 after SNL again resulted in the relief of neuropathic pain in a dose-dependent manner, as indicated by the findings that 10 mg DI only reduces PWF to the stimulation of 0.4 g and PWL to thermal stimulation, whereas 20 mg DI relieved all these neuropathic pain symptoms (Figure 3, B-D). The absence of out-lasting analgesic effect may be related to the rapid metabolism of itaconate (35, 36), which requires DI to be provided continuously. The mechanical and heat thresholds in the contralateral side were not altered (Figure S2, A-

C). The above results demonstrated that DI can prevent and relieve neuropathic pain when given before and after nerve injury, respectively.

3. *DI regulated neuroinflammation in DRGs and spinal dorsal horn of SNL model mice.*

Neuroinflammation in the PNS and CNS has been strongly involved in the development and maintenance of neuropathic pain (37). The L4 DRGs and spinal dorsal horn were harvested on day 10 after DI injection (Figure 4A). Quantitative PCR (qPCR) revealed that SNL led to upregulation of *Il1b* and downregulation of *Il10* in the ipsilateral L4 DRGs. The administration of DI reversed the expression of these factors (Figure 4, B and C). The effect of i.p. DI on neuroinflammation in spinal dorsal horn including activation of glial cells and expression of inflammatory cytokines was further detected. SNL caused increases in the expression of IBA-1 and GFAP in the ipsilateral spinal dorsal horn evidenced by the increase of immunofluorescence (Figure 4, D-F). Western blotting results also demonstrated that SNL increased the protein expression of GFAP in the L4 spinal cord dorsal horn. These glial changes were attenuated by treatment with DI at the dose of 10 mg or 20 mg (Figure 4G). qPCR results demonstrated that SNL induced the upregulation of *Il1b* and *tnf* mRNA and downregulation of *Il10* mRNA in the L4 spinal dorsal horn, all of which were reversed by DI (Figure 4, H-J). Therefore, DI effectively inhibited neuroinflammation in the DRGs and spinal cord of SNL-induced neuropathic pain in mice.

4. *DI inhibited the phosphorylation of ERK1/2 and promoted the Nrf2 level in the DRGs and spinal dorsal horn.*

It is well recognized that nerve injury exerts molecular changes in the DRGs and spinal cord. The mitogen-activated protein kinase (MAPK) signaling pathway, as one of the better-characterized molecular pathways, which is critical in developing and maintaining chronic hypersensitivity (38). A subgroup of the MAPK, ERK1/2, plays an important role in the induction and maintenance of neuropathic pain (39). To investigate whether DI inhibits the phosphorylation of ERK1/2, the expression levels of p-ERK1/2 in the DRGs and spinal dorsal horn was examined after day 10 of injection (day 14 after SNL) in the sham, SNL, SNL+PBS, SNL+DI (10 mg) and SNL+DI (20 mg) groups (Figure 5A). we found that DI, either at the dose of 10 mg or 20mg, inhibited SNL-induced p-ERK1/2 expression in the L4 DRGs (Figure 5, B and D). There were similar results in the spinal cord dorsal horn. Although there was only a tendency for 10 mg, DI at 20 mg significantly suppressed p-ERK1/2 upregulation caused by SNL (Figures 5, C and E).

Itaconate contains an electrophilic α, β-unsaturated carboxylic acids, which may alkylate protein cysteine residues through a Michael addition reaction to form 2,3-dicarboxypropyl adducts. The cysteine alkylated protein KEAP1 usually binds to Nrf2 and promotes its degradation, but the alkylation of KEAP1 cysteine residue allows Nrf2 to activate a transcriptional antioxidants and anti-inflammatory programs (18, 40). Besides, it has been shown that itaconate is required for the activation of anti-inflammatory transcription factor Nrf2 by LPS in mouse and human macrophages (28). Therefore, we further examined whether DI affects Nrf2 expression in SNL model. It was found that SNL model blocked the Nrf2 expression in the DRGs and spinal dorsal horn, but the treatment of DI promoted the production of Nrf2 in a dose-dependent manner in SNL mice (Figure 5, F-I). SNL surgery did not change the ERK1/2 phosphorylation

and Nrf2 expression in the contralateral spinal dorsal horn (Figure S3, A-D). However, DI boosted levels of Nrf2 protein in the contralateral spinal dorsal horn (Figure S3, B and D). These results demonstrated that DI suppressed the phosphorylation of ERK1/2 and influenced the Nrf2 expression in the DRGs and spinal dorsal horn in SNL model.

5. *DI inhibited inflammatory cytokine production and enhanced Nrf2 expression in cultured microglia.*

The regulatory effects of itaconate on peripheral macrophages have been well established (28), there are few studies of its effect on microglia. Microglia, as resident macrophage in the CNS, composes the innate immune system of the CNS and is a key cellular mediators of neuroinflammatory processes (41). In Figure 4D, it has been certified that DI can inhibit microglial activation in the spinal dorsal horn. However, the anti-inflammatory consequence of this inhibition requires verification. Therefore, we did in vitro experiments on microglial cell line BV_2. Firstly, microglial cells (1×10^6 cells) pretreated with DI (250 μM) for 12 h were stimulated by LPS (100 ng/ml) for 2 h, then the cells were collected for RT-PCR and western blot (Figure 6A). As demonstrated in Figure 6B and C, DI significantly reduced the contents of *Il1b* and *tnf* mRNA in BV_2 cells exposed to LPS. Besides, we examined the expression of Nrf2 in BV_2 cells. The stimulation of LPS or exposure of DI alone improved the level of Nrf2 of microglia, but the co-administration of LPS and DI promoted more production of Nrf2 (Figure 6, D and E).

To further verify the role of Nrf2 in the inhibition of microglia activation by DI, we treated BV_2 cells with a specific *irg1* siRNA (4 μl) for 6 h. It has been shown that suppression of IRG1 expression that could inhibited the production of itaconate (28). This treatment resulted in a 67% reduction in *irg*1 production (Figure 6F), which led to a reduction in Nrf2 expression in BV_2 cells compared with control siRNA (con-siRNA) treatment (Figure 6, G and H). The inflammatory factors *Il1b* and *tnf* were increased after the treatment of irg1 siRNA, which was reversed by DI, although there was no difference between LPS plus irg1-siRNA group and LPS plus irg1-siRNA plus DI group, which demonstrated that exogenous itaconate derivative like DI, may have a certain effect on endogenous itaconate, even though DI could not simulate the endogenous itaconate. In addition, there was significant difference between LPS plus con-siRNA group and LPS plus con-siRNA plus DI group (Figure 6, I and J).

6. *DI alleviated CFA-induced inflammatory pain.*

In addition to neuropathic pain model, we verified the analgesic efficacy of DI (20 mg) in the inflammatory pain model that was induced by CFA (20μL) via the plantar injection. Pain behavior was evaluated at baseline, 2h, 6h, 1, 2, 4, 6, 8 and 12 day after CFA injection (Figure 7A). In this model, mechanical allodynia and thermal hyperalgesia were rapidly induced within 2 h and peaks at 1 day and began to decrease from day 2 after CFA in mice (Figure 7, B-D). The continuous administration of DI (20 mg), given day 1 after CFA, produced an inhibition of CFA-induced mechanical and thermal painful behaviors (Figure 7, B-D). The sensitivity to mechanical and thermal stimulations on the contralateral side were not altered (Figure S4, A-C). These results demonstrated that the analgesic effect of DI is evident not only in the neuropathic pain but also the inflammatory pain.

7. *DI inhibited inflammation response in the spinal cord and peripheral tissues of CFA model mice.*

Inflammatory pain occurs during inflammatory or immune responses. The pro-inflammatory mediators (e.g., cytokines) modulate pain sensitivity, and the accumulation of infiltrated cells induces the development of peripheral and central sensitization in the chronic pain conditions (42). PCR results revealed that CFA also caused upregulation of *Il1b* and *tnf* in the ipsilateral hind paw and L4–L5 spinal dorsal horn, and downregulation of *Il10* in the ipsilateral hind paw (Figure 8, A-E). The expression changes of these mRNAs were reserved by treatment with DI (Figure 8, A-E). H&E staining result showed that the vehicle group had normal paw tissue, whereas the hind paws that received CFA injection showed massive accumulation of infiltrated cells (Figure 8F). However, infiltrated inflammatory cell was evidently decreased by DI treatment (20 mg) on CFA day 5. This result verified that DI also inhibited inflammation response in the spinal cord and hind paw tissue of CFA model mice.

Discussion

Itaconate, as a metabolite, is generated by mitochondria-associated enzyme IRG1, has recently been regarded as a regulator of macrophage activation (19, 29). It has been shown that itaconate exerts an anti-inflammatory effect through promoting Nrf2 or suppressing SDH which exerts anti-oxidant, anti-inflammatory and immunomodulatory effects (18). A number of studies reported the therapeutic effect with DI administration in rodent no matter it is systemic or local injection, but the analgesic effects are not clear. Therefore, in this study, our findings firstly demonstrate that a continuous i.p. injection of different doses of DI (10mg or 20mg), either at pre-SNL time points (3 days before SNL) or at post-SNL time points (28 days after SNL), produced relief from neuropathic pain symptoms, including mechanical allodynia and heat hyperalgesia in mice. However, different administration time of DI leads to different pain relief effects. In Fig. 2, a continuous i.p. injection of DI, given starting from day 4 to 32 after SNL, produced long-term relief (> 4 weeks) of SNL-induced painful behaviors following either low dose (10mg) or high dose (20mg), which has the similar result with the inflammatory pain model caused by CFA. In previous studies, in addition to postoperative administration, DI can also be administered before the establishment of the model (24). Therefore, we tried continuous administration of DI from 3 days before the model establishment until the 3 days after SNL surgery, and found that only large doses of DI (20mg) slightly alleviated mechanical and thermal pain caused by SNL. The analgesic effect of DI would disappear after the drug was stopped. Then SNL-induced neuropathic pain was reversed when DI was provided again, as seen in Fig. 3, which this difference may be closely related to the rapid metabolism of itaconate (17).

DI treatment reduced central and peripheral inflammation response in spinal cord, DRGs and hind paws tissues, and also suppressed the phosphorylation of ERK1/2, as an important cellular molecule related to pain sensitization, in the DRGs and spinal dorsal horn. Our results demonstrate the immunomodulatory effect of DI on SNL/CFA-induced pain. Besides, LPS to stimulate the microglia mimics the pathological change in vivo. This is consistent with in vivo experiment that DI exhibited reduced inflammatory cytokines.

In this study, we found that SNL inhibited the expression of Nrf2 in the DRGs and spinal dorsal horn, which has the same result with that of Wei Di (43). But in vitro experiment, it was shown that the expression of Nrf2 was upregulated after LPS simulation, which demonstrated that after the initial injury, the body produced anti-inflammatory or analgesic substances to protect itself from injury, such as increased Nrf2 in cells, but this increase cannot completely eliminate the injury, which need to be provided exogenously. The production of Nrf2 pretreated with irg1 siRNA were compromised in the microglia. The administration of exogenous DI potently reversed inflammatory response induced by LPS. Nrf2 is a key transcription factor in the regulation of multiple antioxidants (44). Kawamura *et al*. have proved that inhaled hydrogen reduced lung injury by activating Nrf2 mediates oxidative stress response mechanisms (45, 46). Studies have demonstrated that activation of the Nrf2 protected against inflammation-mediated tissue damage by inhibiting the production of proinflammatory mediators (47, 48). Johnson *et al*. have shown that the absence of Nrf2 exacerbates the pathogenic process of EAE in mice (49, 50). Wei Di *et al*. have demonstrated that the activation of the Nrf2 alleviates the nitroglycerin-induced hyperalgesia in rats (43). Itaconate exerts its therapeutic role in many diseases by regulating the expression of Nrf2. For example, Nrf2-signaling revealed potent antiviral of 4-octyl-itaconate in COVID-19 (51). Itaconate prevented abdominal aortic aneurysm formation through activating Nrf2 to inhibit inflammation (26). Itaconate activated Nrf2 in hepatocytes to protect against liver ischemia-reperfusion injury and exhibited immunomodulatory effects in EAE (22, 28) and so on. Therefore, provided several lines of evidence have demonstrate that Nrf2 may play an important role in the analgesic effects of DI. It would need to investigate further whether DI-induced Nrf2 activation has a direct effect on the relief of chronic pain in vivo. In addition to Nrf2, whether the inhibition of SDH is also involved in the analgesic effect of DI, which need to be further explored.

Apart from DI, 4-octyl itaconate (4-OI) is regarded as another common derivative of itaconate. It was found that DI degrades rapidly in cells, without causing the release of itaconate, indicating that it is unlikely to mimic endogenous itaconate. OI has been determined to form endogenous itaconate, making it a suitable cell-permeable itaconate surrogate. Two types of itaconate derivatives both can effectively activate Nrf2 signaling to exert their anti-inflammatory and antioxidant properties (17). Its toxicity is likely to be very low, given that itaconate is produced in the course of a natural immune response, (52). Therefore, modifying of itaconate derivatives to delay the rate of metabolism in the body and prolong its therapeutic effect or endogenous form (for example, by boosting IRG1 activity) may bring good news to clinical patients in the future.

Conclusions

In summary, we reported for the first time that continuously i.p. injected DI not only produce neuropathic pain relief in mice and ameliorated inflammatory pain. In addition, we identified that DI suppressed neuroinflammation and the phosphorylation of ERK1/2 in the peripheral and central tissues, and ameliorated inflammatory response in the microglia. DI also promoted the Nrf2 expression, suggesting that DI elicits sustained chronic pain relief, which will be developed as a novel therapeutic agent for the treatment of chronic pain.

List Of Abbreviations

DI Dimethyl itaconate

Nrf2 Nuclear factor-erythroid 2 p45-related factor 2

IRG1 Immune-responsive gene 1

TNF-α Tumor necrosis factor-alpha

IL-1β Interleukin-1β

NO Nitric oxide

DRGs Dorsal root ganglion

SDH Succinate dehydrogenase

CFA Complete Freund's adjuvant

SNL Spinal nerve ligation

PWF Paw withdrawal frequencies

PWL Paw withdrawal latencies

PNS Peripheral nervous system

CNS Central Nervous System

MAPK Mitogen-activated protein kinase

4-OI 4-octyl itaconate

Declarations

Acknowledgements

Thanks to Department of Neurosurgery, The Second Affiliated Hospital of Zhejiang University School of Medicine for providing microglia.

Author’s contributions

JXR and LNY conceived the experiments. JXR, LNY and JQL contributed to design experiments. JQL, LFM and DSG perform experiments. NS, YL and LLF contributed to data analysis. JXR, ZZC and KS

contributed to study discussion and manuscript editing. MY contributed to the assessment and write the manuscript. All authors read and approved the final manuscript.

Funding

This work is supported by National Natural Science Foundation of China (82071227 and 81771189) and partly supported by the and the Natural Science Foundation of Zhejiang Province (LQ19C090006, LY18H090006, LZ18H090001).

Availability of data and materials

The datasets of the current study are available from the corresponding author on a reasonable request.

Ethics approval and consent to participate

This study was carried out in accordance with the National Institute of Health Guide for the Care and Use of Laboratory Animals. All experimental procedures were approved by the Animal Research Committee of the Second Affiliated Hospital, School of Medicine, Zhejiang University (Hangzhou, China).

Consent for publication

Not applicable.

Competing interests

All authors claim that there are no conflicts of interest.

References

1. Ren JX, Liu N, Sun N, Zhang KH, Yu LN. Mesenchymal Stem Cells and their Exosomes: Promising Therapeutics for Chronic Pain. *Current Stem Cell Research & Therapy* 2019,14(8):644-653.
2. Huh Y, Ji RR, Chen G. Neuroinflammation, Bone Marrow Stem Cells, and Chronic Pain. *Front Immunol* 2017,8:1014.
3. Ji RR, Nackley A, Huh Y, Terrando N, Maixner W. Neuroinflammation and Central Sensitization in Chronic and Widespread Pain. *Anesthesiology* 2018,129(2):343-366.
4. Pizzo PA, Clark NM. Alleviating Suffering 101-Pain Relief in the United States. *New England Journal of Medicine* 2012,366(3):197-199.
5. Gereau RWt, Sluka KA, Maixner W, Savage SR, Price TJ, Murinson BB, Sullivan MD, Fillingim RB. A pain research agenda for the 21st century. *J Pain* 2014,15(12):1203-1214.
6. Sayo A, Konishi H, Kobayashi M, Kano K, Kobayashi H, Hibi H, Aoki J, Kiyama H. GPR34 in spinal microglia exacerbates neuropathic pain in mice. *J Neuroinflammation* 2019,16(1):82.

7. Ji RR, Xu ZZ, Gao YJ. Emerging targets in neuroinflammation-driven chronic pain. *Nat Rev Drug Discov* 2014,13(7):533-548.
8. Shiue SJ, Rau RH, Shiue HS, Hung YW, Li ZX, Yang KD, Cheng JK. Mesenchymal stem cell exosomes as a cell-free therapy for nerve injury-induced pain in rats. *Pain* 2019,160(1):210-223.
9. Kalynovska N, Diallo M, Sotakova-Kasparova D, Palecek J. Losartan attenuates neuroinflammation and neuropathic pain in paclitaxel-induced peripheral neuropathy. *J Cell Mol Med* 2020,24(14):7949-7958.
10. McMahon SB, Cafferty WBJ, Marchand F. Immune and glial cell factors as pain mediators and modulators. *Experimental Neurology* 2005,192(2):444-462.
11. Ji RR, Chamessian A, Zhang YQ. Pain regulation by non-neuronal cells and inflammation. *Science* 2016,354(6312):572-577.
12. Zhang X, Hartung JE, Bortsov AV, Kim S, O'Buckley SC, Kozlowski J, Nackley AG. Sustained stimulation of beta(2)- and beta(3)-adrenergic receptors leads to persistent functional pain and neuroinflammation. *Brain Behavior and Immunity* 2018,73:520-532.
13. Paladini A, Fusco M, Cenacchi T, Schievano C, Piroli A, Varrassi G. Palmitoylethanolamide, a Special Food for Medical Purposes, in the Treatment of Chronic Pain: A Pooled Data Meta-analysis. *Pain Physician* 2016,19(2):11-24.
14. Gao YJ, Ji RR. Chemokines, neuronal-glial interactions, and central processing of neuropathic pain. *Pharmacol Ther* 2010,126(1):56-68.
15. Hooftman A, O'Neill LAJ. The Immunomodulatory Potential of the Metabolite Itaconate. *Trends Immunol* 2019,40(8):687-698.
16. Hooftman A, Angiari S, Hester S, Corcoran SE, Runtsch MC, Ling C, Ruzek MC, Slivka PF, McGettrick AF, Banahan K, Hughes MM, Irvine AD, Fischer R, O'Neill LAJ. The Immunomodulatory Metabolite Itaconate Modifies NLRP3 and Inhibits Inflammasome Activation. *Cell Metab* 2020,32(3):468-478 e467.
17. Sun X, Zhang B, Pan X, Huang H, Xie Z, Ma Y, Hu B, Wang J, Chen Z, Shi P. Octyl itaconate inhibits osteoclastogenesis by suppressing Hrd1 and activating Nrf2 signaling. *FASEB J* 2019,33(11):12929-12940.
18. Mills EL, Ryan DG, Prag HA, Dikovskaya D, Menon D, Zaslona Z, Jedrychowski MP, Costa ASH, Higgins M, Hams E, Szpyt J, Runtsch MC, King MS, McGouran JF, Fischer R, Kessler BM, McGettrick AF, Hughes MM, Carroll RG, Booty LM, Knatko EV, Meakin PJ, Ashford MLJ, Modis LK, Brunori G, Sevin DC, Fallon PG, Caldwell ST, Kunji ERS, Chouchani ET, Frezza C, Dinkova-Kostova AT, Hartley RC, Murphy MP, O'Neill LA. Itaconate is an anti-inflammatory metabolite that activates Nrf2 via alkylation of KEAP1. *Nature* 2018,556(7699):113-+.
19. Cordes T, Wallace M, Michelucci A, Divakaruni AS, Sapcariu SC, Sousa C, Koseki H, Cabrales P, Murphy AN, Hiller K, Metallo CM. Immunoresponsive Gene 1 and Itaconate Inhibit Succinate Dehydrogenase to Modulate Intracellular Succinate Levels. *J Biol Chem* 2016,291(27):14274-14284.

20. Lampropoulou V, Sergushichev A, Bambouskova M, Nair S, Vincent EE, Loginicheva E, Cervantes-Barragan L, Ma X, Huang SC, Griss T, Weinheimer CJ, Khader S, Randolph GJ, Pearce EJ, Jones RG, Diwan A, Diamond MS, Artyomov MN. Itaconate Links Inhibition of Succinate Dehydrogenase with Macrophage Metabolic Remodeling and Regulation of Inflammation. *Cell Metab* 2016,24(1):158-166.
21. Yu XH, Zhang DW, Zheng XL, Tang CK. Itaconate: an emerging determinant of inflammation in activated macrophages. *Immunol Cell Biol* 2019,97(2):134-141.
22. Yi Z, Deng M, Scott MJ, Fu G, Loughran PA, Lei Z, Li S, Sun P, Yang C, Li W, Xu H, Huang F, Billiar TR. Immune-Responsive Gene 1/Itaconate Activates Nuclear Factor Erythroid 2-Related Factor 2 in Hepatocytes to Protect Against Liver Ischemia-Reperfusion Injury. *Hepatology* 2020,72(4):1394-1411.
23. Ogger PP, Albers GJ, Hewitt RJ, O'Sullivan BJ, Powell JE, Calamita E, Ghai P, Walker SA, McErlean P, Saunders P, Kingston S, Molyneaux PL, Halket JM, Gray R, Chambers DC, Maher TM, Lloyd CM, Byrne AJ. Itaconate controls the severity of pulmonary fibrosis. *Sci Immunol* 2020,5(52).
24. Cordes T, Lucas A, Divakaruni AS, Murphy AN, Cabrales P, Metallo CM. Itaconate modulates tricarboxylic acid and redox metabolism to mitigate reperfusion injury. *Mol Metab* 2020,32:122-135.
25. Zhang D, Lu Z, Zhang Z, Man J, Guo R, Liu C, Wang J. A likely protective effect of dimethyl itaconate on cerebral ischemia/reperfusion injury. *Int Immunopharmacol* 2019,77:105924.
26. Song HY, Xu T, Feng XF, Lai YX, Yang Y, Zheng H, He X, Wei GQ, Liao WJ, Liao YL, Zhong LT, Bin JP. Itaconate prevents abdominal aortic aneurysm formation through inhibiting inflammation via activation of Nrf2. *Ebiomedicine* 2020,57.
27. Zhang S, Jiao Y, Li C, Liang X, Jia H, Nie Z, Zhang Y. Dimethyl Itaconate Alleviates the Inflammatory Responses of Macrophages in Sepsis. *Inflammation* 2021,44(2):549-557.
28. Kuo PC, Weng WT, Scofield BA, Paraiso HC, Brown DA, Wang PY, Yu IC, Yen JH. Dimethyl itaconate, an itaconate derivative, exhibits immunomodulatory effects on neuroinflammation in experimental autoimmune encephalomyelitis. *J Neuroinflammation* 2020,17(1):138.
29. Bambouskova M, Gorvel L, Lampropoulou V, Sergushichev A, Loginicheva E, Johnson K, Korenfeld D, Mathyer ME, Kim H, Huang LH, Duncan D, Bregman H, Keskin A, Santeford A, Apte RS, Sehgal R, Johnson B, Amarasinghe GK, Soares MP, Satoh T, Akira S, Hai T, de Guzman Strong C, Auclair K, Roddy TP, Biller SA, Jovanovic M, Klechevsky E, Stewart KM, Randolph GJ, Artyomov MN. Electrophilic properties of itaconate and derivatives regulate the IkappaBzeta-ATF3 inflammatory axis. *Nature* 2018,556(7702):501-504.
30. Vilceanu D, Honore P, Hogan QH, Stucky CL. Spinal nerve ligation in mouse upregulates TRPV1 heat function in injured IB4-positive nociceptors. *J Pain* 2010,11(6):588-599.
31. Sun S, Yin Y, Yin X, Cao F, Luo D, Zhang T, Li Y, Ni L. Anti-nociceptive effects of Tanshinone IIA (TIIA) in a rat model of complete Freund's adjuvant (CFA)-induced inflammatory pain. *Brain Res Bull* 2012,88(6):581-588.
32. Chen G, Park CK, Xie RG, Ji RR. Intrathecal bone marrow stromal cells inhibit neuropathic pain via TGF-beta secretion. *Journal of Clinical Investigation* 2015,125(8):3226-3240.

33. Huang LN, Zou Y, Wu SG, Zhang HH, Mao QX, Li JB, Tao YX. Fn14 Participates in Neuropathic Pain Through NF-kappa B Pathway in Primary Sensory Neurons. *Molecular Neurobiology* 2019,56(10):7085-7096.
34. Kawasaki Y, Xu ZZ, Wang X, Park JY, Zhuang ZY, Tan PH, Gao YJ, Roy K, Corfas G, Lo EH, Ji RR. Distinct roles of matrix metalloproteases in the early- and late-phase development of neuropathic pain. *Nat Med* 2008,14(3):331-336.
35. Adler J, Wang SF, Lardy HA. The metabolism of itaconic acid by liver mitochondria. *J Biol Chem* 1957,229(2):865-879.
36. Wang SF, Adler J, Lardy HA. The pathway of itaconate metabolism by liver mitochondria. *J Biol Chem* 1961,236:26-30.
37. Ellis A, Bennett DL. Neuroinflammation and the generation of neuropathic pain. *Br J Anaesth* 2013,111(1):26-37.
38. Landry RP, Martinez E, DeLeo JA, Romero-Sandoval EA. Spinal cannabinoid receptor type 2 agonist reduces mechanical allodynia and induces mitogen-activated protein kinase phosphatases in a rat model of neuropathic pain. *J Pain* 2012,13(9):836-848.
39. Xie J, Ren J, Liu N, Wu C, Xiao D, Luo H, Du J. Pretreatment with AM1241 Enhances the Analgesic Effect of Intrathecally Administrated Mesenchymal Stem Cells. *Stem Cells Int* 2019,2019:7025473.
40. Arruri VK, Gundu C, Kalvala AK, Sherkhane B, Khatri DK, Singh SB. Carvacrol abates NLRP3 inflammasome activation by augmenting Keap1/Nrf-2/p62 directed autophagy and mitochondrial quality control in neuropathic pain. *Nutr Neurosci* 2021:1-16.
41. Subhramanyam CS, Wang C, Hu Q, Dheen ST. Microglia-mediated neuroinflammation in neurodegenerative diseases. *Semin Cell Dev Biol* 2019,94:112-120.
42. Park J, Kim YT. Erythronium japonicum Alleviates Inflammatory Pain by Inhibiting MAPK Activation and by Suppressing NF-kappaB Activation via ERK/Nrf2/HO-1 Signaling Pathway. *Antioxidants (Basel)* 2020,9(7).
43. Di W, Shi X, Lv H, Liu J, Zhang H, Li Z, Fang Y. Activation of the nuclear factor E2-related factor 2/anitioxidant response element alleviates the nitroglycerin-induced hyperalgesia in rats. *J Headache Pain* 2016,17(1):99.
44. Zhu W, Ding Y, Kong W, Li T, Chen H. Docosahexaenoic Acid (DHA) Provides Neuroprotection in Traumatic Brain Injury Models via Activating Nrf2-ARE Signaling. *Inflammation* 2018,41(4):1182-1193.
45. Kawamura T, Huang CS, Peng X, Masutani K, Shigemura N, Billiar TR, Okumura M, Toyoda Y, Nakao A. The effect of donor treatment with hydrogen on lung allograft function in rats. *Surgery* 2011,150(2):240-249.
46. Kawamura T, Wakabayashi N, Shigemura N, Huang CS, Masutani K, Tanaka Y, Noda K, Peng X, Takahashi T, Billiar TR, Okumura M, Toyoda Y, Kensler TW, Nakao A. Hydrogen gas reduces hyperoxic lung injury via the Nrf2 pathway in vivo. *Am J Physiol Lung Cell Mol Physiol* 2013,304(10):L646-656.

47. Dong F, Wang S, Wang Y, Yang X, Jiang J, Wu D, Qu X, Fan H, Yao R. Quercetin ameliorates learning and memory via the Nrf2-ARE signaling pathway in d-galactose-induced neurotoxicity in mice. *Biochem Biophys Res Commun* 2017,491(3):636-641.
48. Kim J, Cha YN, Surh YJ. A protective role of nuclear factor-erythroid 2-related factor-2 (Nrf2) in inflammatory disorders. *Mutat Res* 2010,690(1-2):12-23.
49. Liu Y, Dong F, Guo R, Zhang Y, Qu X, Wu X, Yao R. Hydrogen-Rich Saline Ameliorates Experimental Autoimmune Encephalomyelitis in C57BL/6 Mice Via the Nrf2-ARE Signaling Pathway. *Inflammation* 2019,42(2):586-597.
50. Johnson DA, Amirahmadi S, Ward C, Fabry Z, Johnson JA. The absence of the pro-antioxidant transcription factor Nrf2 exacerbates experimental autoimmune encephalomyelitis. *Toxicol Sci* 2010,114(2):237-246.
51. Olagnier D, Farahani E, Thyrsted J, Blay-Cadanet J, Herengt A, Idorn M, Hait A, Hernaez B, Knudsen A, Iversen MB, Schilling M, Jorgensen SE, Thomsen M, Reinert LS, Lappe M, Hoang HD, Gilchrist VH, Hansen AL, Ottosen R, Nielsen CG, Moller C, van der Horst D, Peri S, Balachandran S, Huang J, Jakobsen M, Svenningsen EB, Poulsen TB, Bartsch L, Thielke AL, Luo Y, Alain T, Rehwinkel J, Alcami A, Hiscott J, Mogensen TH, Paludan SR, Holm CK. SARS-CoV2-mediated suppression of NRF2-signaling reveals potent antiviral and anti-inflammatory activity of 4-octyl-itaconate and dimethyl fumarate. *Nat Commun* 2020,11(1):4938.
52. O'Neill LAJ, Artyomov MN. Itaconate: the poster child of metabolic reprogramming in macrophage function. *Nature Reviews Immunology* 2019,19(5):273-281.

Figures

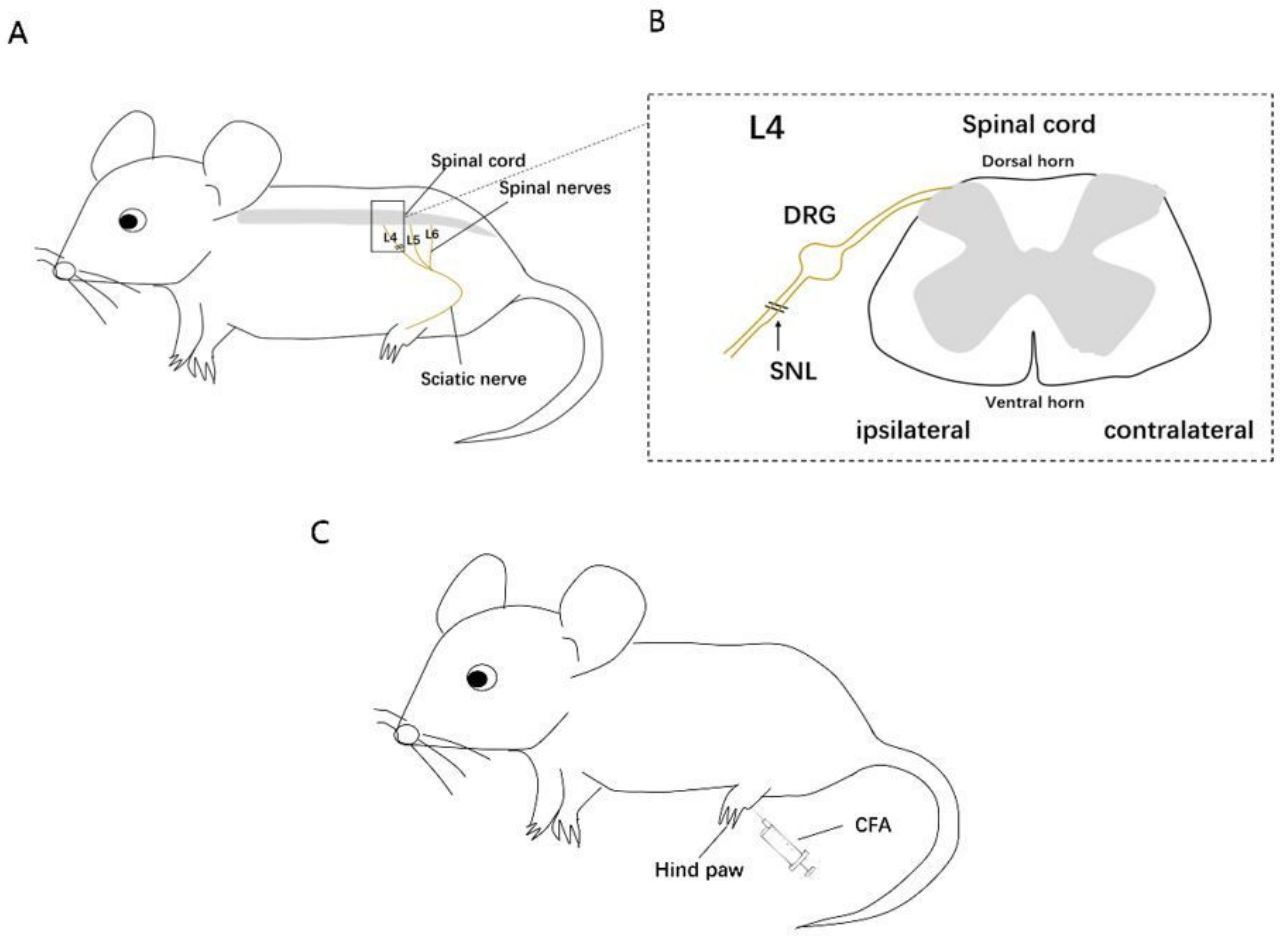

Figure 1

Schematic summary of L4 SNL pain model and CFA-induced inflammatory pain model. (A-B) The L4 SNL pain model cartoon for this study. The left L4 spinal nerves were ligated to induce neuropathic pain. (C) The inflammatory pain model cartoon caused by CFA for this study. The left hind paw of mice was injected by CFA.

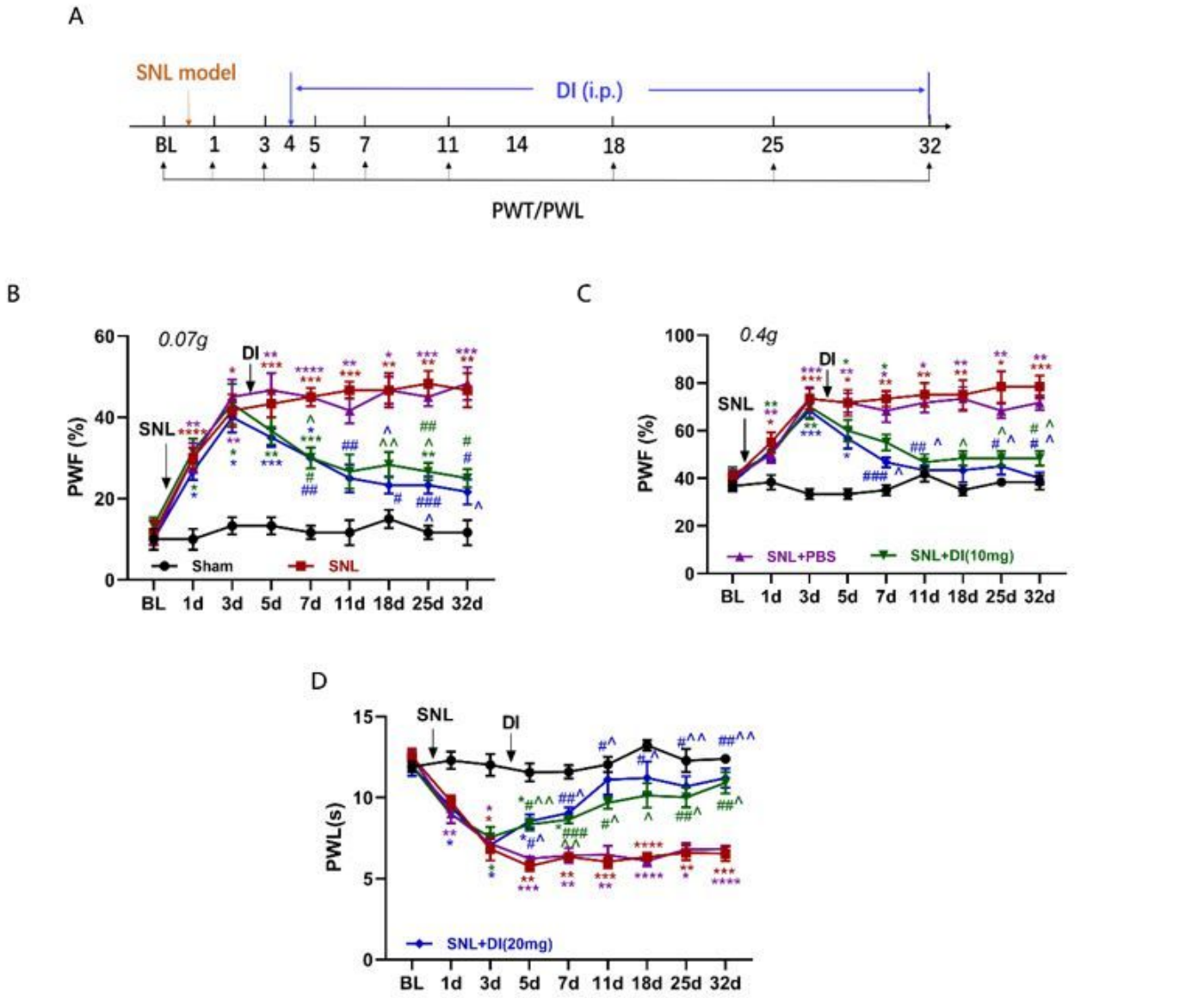

Figure 2

DI alleviated neuropathic pain. (A) Paradigm showing the experimental procedures. (B-D) DI (10 mg or 20 mg), given day 4 after SNL, reduced PWF (B and C) and increases PWL (D). *p < 0.05, **p < 0.01, ***p < 0.001 and ****p < 0.0001 versus the Sham group; #p < 0.05, ##p < 0.01, and ###p < 0.001 versus the SNL group; ∧p < 0.05 and ∧∧p < 0.01 versus the SNL+PBS group; n = 6 mice/group. Arrows in (B-D) indicate the time of SNL model establishment and DI injection. BL, baseline.

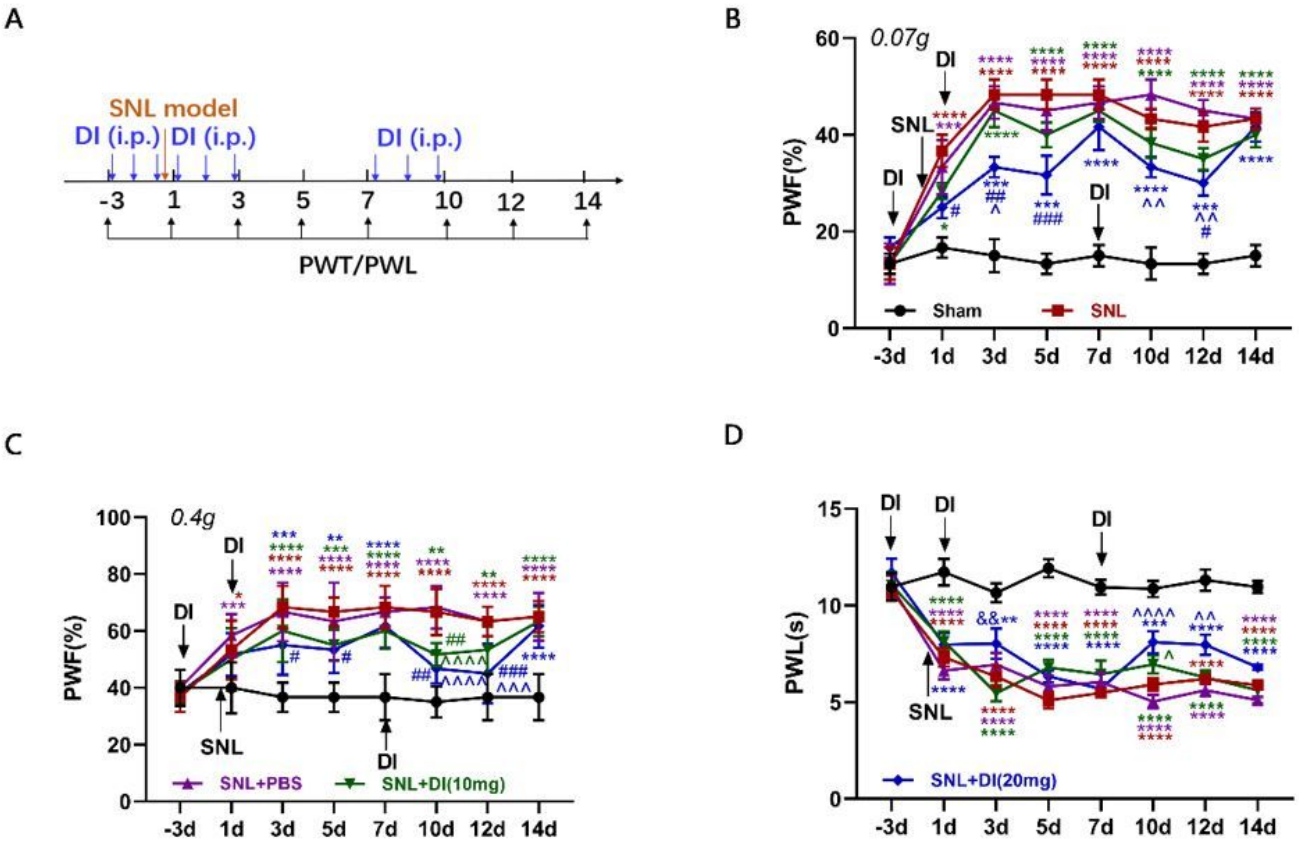

Figure 3

DI prevented neuropathic pain. (A) Paradigm showing the experimental procedures. (B-D) DI, given 3 days before and after SNL model and day 7 to 10 after SNL, reduced PWF (B and C) and increases PWL (D) in the dose-dependent manner. *p < 0.05, **p < 0.01, ***p < 0.001 and ****p < 0.0001 versus the Sham group; #p < 0.05, ##p < 0.01 and ###p < 0.001 versus the SNL group; ∧p < 0.05, ∧∧p < 0.01, ∧∧∧p < 0.001 and ∧∧∧∧p < 0.0001versus the SNL+PBS group; &&p < 0.01 versus the SNL+DI (10mg) group; n = 6 mice/group. Arrows in (B-D) indicate the time of SNL model establishment and DI injection.

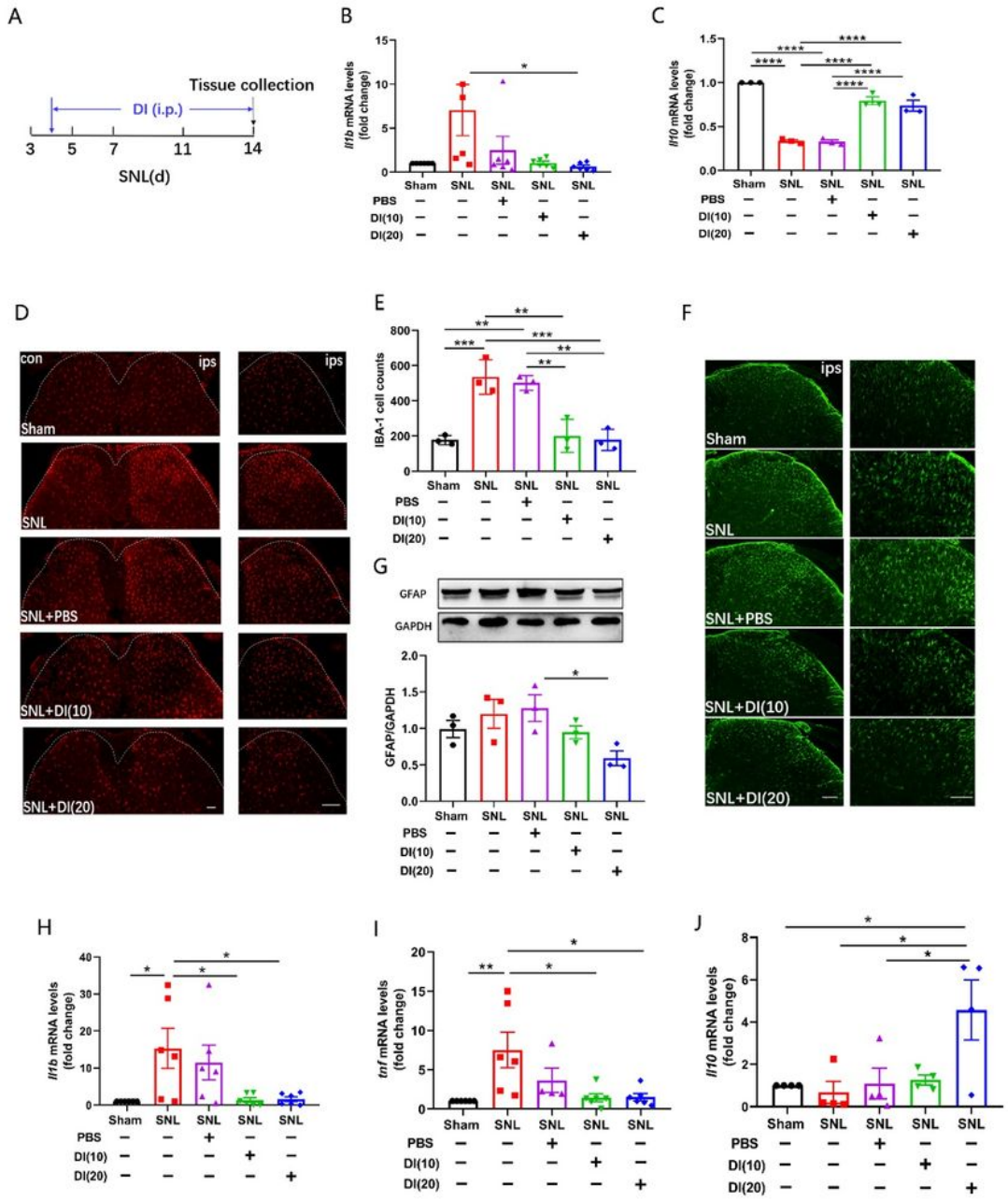

Figure 4

DI inhibited neuroinflammation in the L4 DRGs and spinal dorsal horn. (A) Paradigm showing the timing of DI treatment (SNL day 4) and tissue collection (SNL day 14). (B and C) qPCR showing expression levels of Il1b (B) and Il10 (C) mRNAs in L4 DRGs and the effects of DI, n = 3 mice/group. (D) Inhibition of SNL-induced upregulation of the microglial marker IBA-1 (Red) in L4 spinal dorsal horn by i.p. injection of DI (10mg or 20mg). Scale bar: 400 μm (left) and 200μm (right). (E) Quantification of IBA-1 staining, n = 3

mice/group. Graph in F shows the expression of GFAP staining (Green). Scale bar: 200 μm (left) and 100 μm (right). (G) Western blot showing expression levels of GFAP protein in L4 spinal dorsal horn after the administration of DI, n = 6 mice/group. (H-J) qPCR showing expression levels of Il1b (H), tnf (I) and Il10 (J) mRNAs in L4 spinal cord horn after i.p. DI, n = 4-6 mice/group. *p < 0.05, **p < 0.01, ***p < 0.001 and ****p < 0.0001.

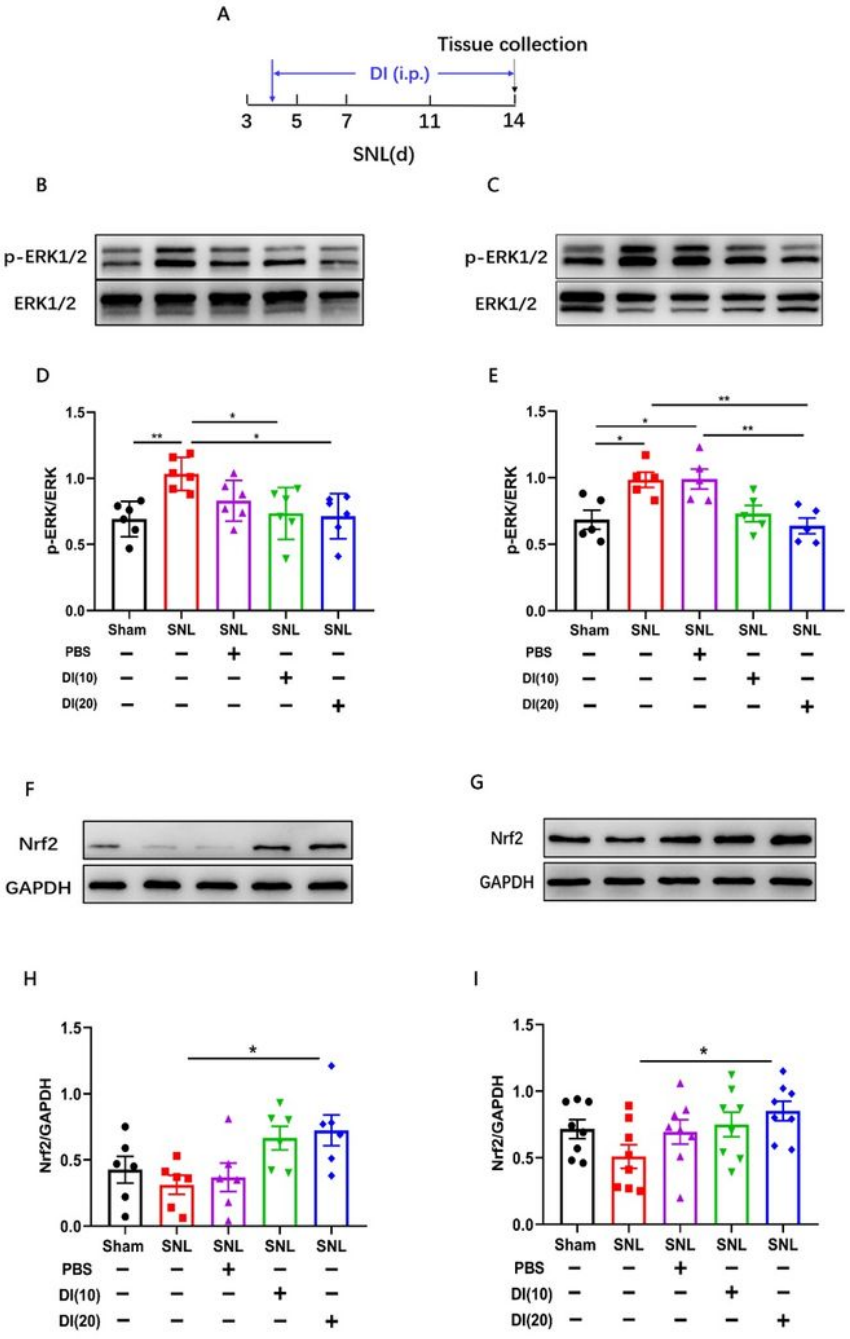

Figure 5

DI inhibited p-ERK1/2 and enhanced Nrf2 in the DRGs and spinal cord dorsal horn. (A) Timeline indicating the time of DI (SNL day 4) and tissue collection (SNL day 14). (B and C) Western blot results of p-ERK1/2 expression after i.p. injection of DI in the DRGs (B) and in the spinal dorsal horn (C) at SNL day 14. (D and E) Quantification of p-ERK1/2 in the DRGs (D) and in the spinal dorsal horn (E). (F and G) Western blot results of Nrf2 after the continuous administration of DI in the ipsilateral DRGs (F) and spinal dorsal horn (G) at SNL day 14. (H and I) Quantification of Nrf2 in the ipsilateral DRGs (H) and spinal dorsal horn (I). ∗p < 0.05 and **p < 0.01. n = 4-8 mice/group.

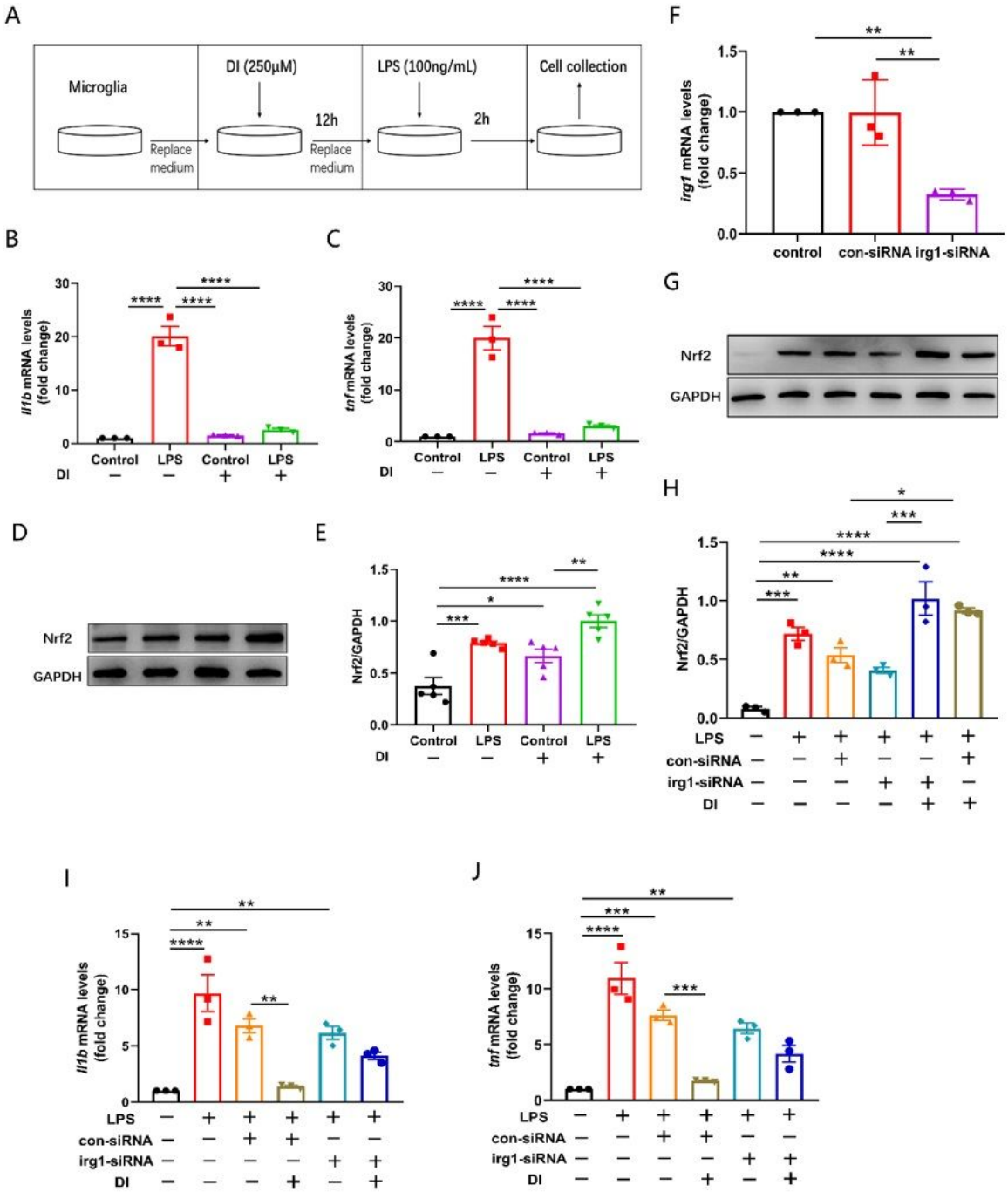

Figure 6

DI inhibited inflammatory response in cultured microglia. (A) Schematic diagram of DI (250μM) and LPS stimulation (100ng/mL) and cell collection. (B-C) PCR analysis showing inhibited Il1b (B) and tnf (C) mRNA after the treatment of DI. (D) WB analysis of Nrf2 expression in the BV2 of four groups. (E) Quantification of Nrf2 protein in the BV2 cells. (F) Inhibition of irg1 mRNA in the BV2 cells with the treatment of irg1 siRNA (4 μl for 6h), but not with control siRNA. (G) WB analysis of Nrf2 expression in the BV2 with intervention of irg1-siRNA, con-siRNA and DI. (H) Quantification of Nrf2 protein in these groups. (I and J) PCR analysis showed that DI inhibited the increase of Il1b (I) and tnf (J) mRNA pretreated with irg1 siRNA. *p < 0.05, **p < 0.01, ***p < 0.001 and ****p < 0.0001. Con-siRNA, control siRNA.

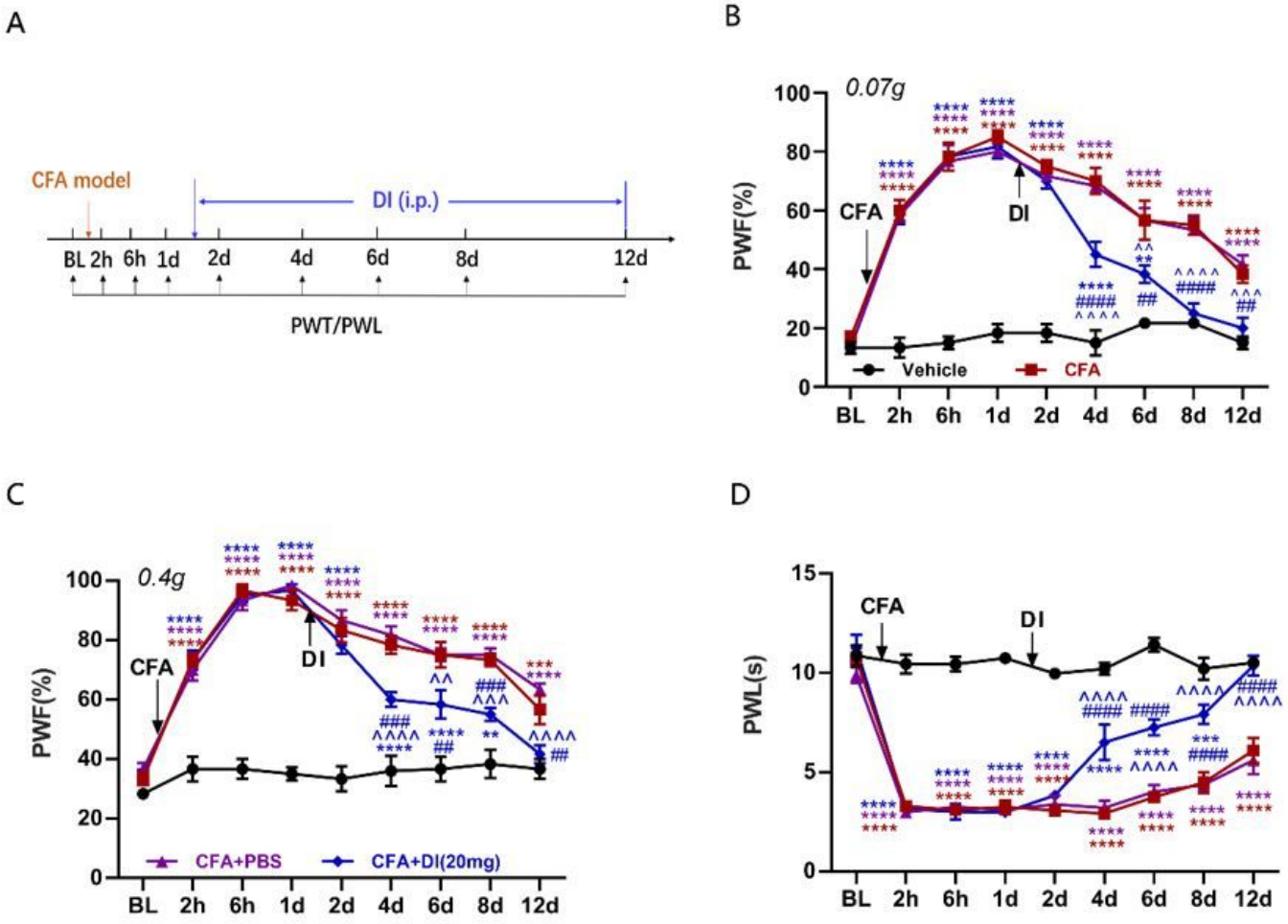

Figure 7

Inhibition of CFA-induced inflammatory pain by DI. (A) Paradigm showing the experimental procedures. (B-D) DI (20mg), given day 1 after CFA injection, reduced PWF (B and C) and increases PWL (D). **p < 0.01, ***p < 0.001 and ****p < 0.0001 versus the Vehicle group; ##p < 0.01, ###p < 0.001 and ####p < 0.0001 versus the CFA group; ^^p < 0.01, ^^^p < 0.001 and ^^^^p < 0.0001 versus the CFA+PBS group; n = 6 mice/group. Arrows in (B-D) indicate the time of CFA model establishment and DI injection. BL, baseline.

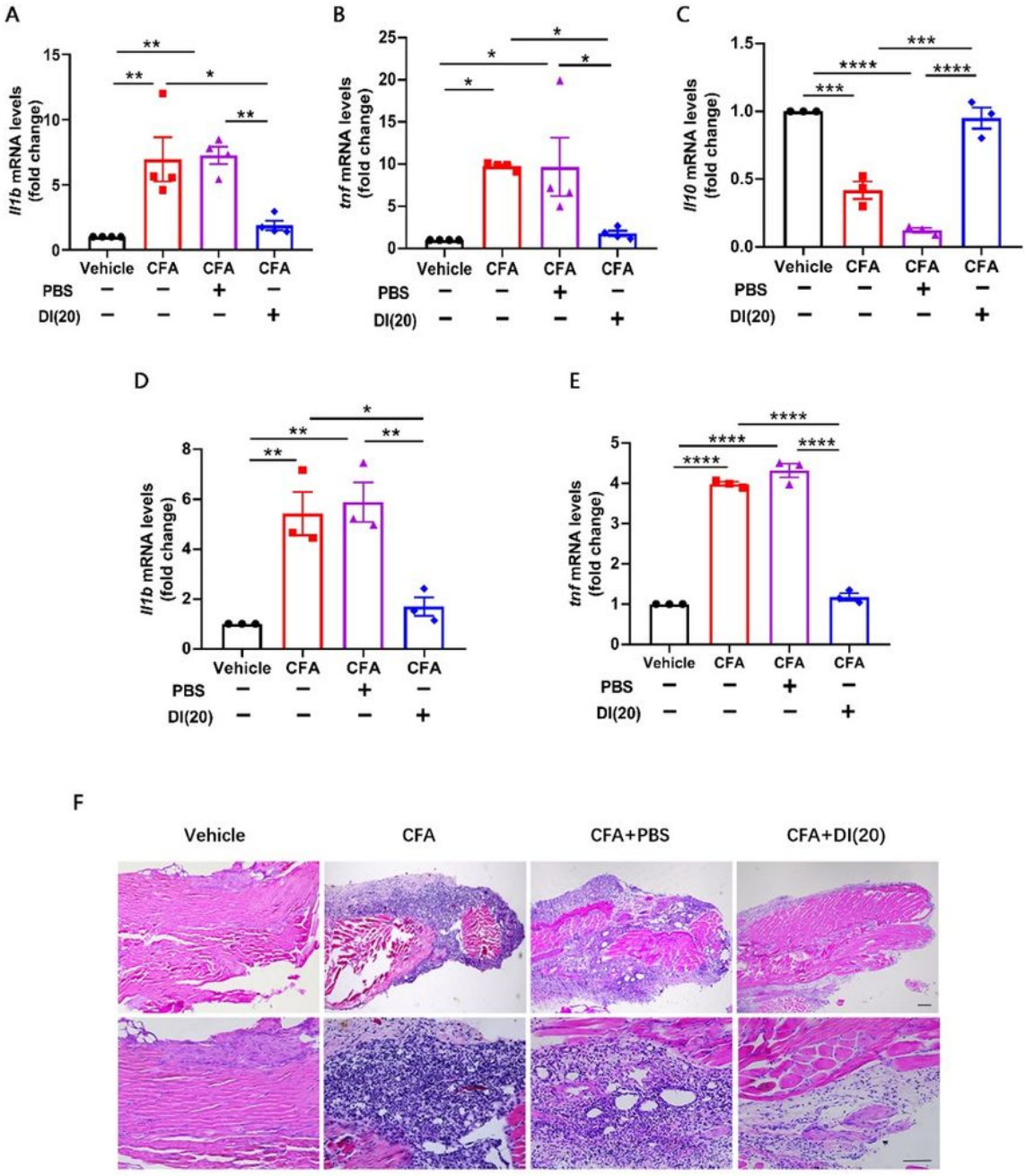

Figure 8

DI inhibit CFA-induced neuroinflammation in spinal cord dorsal horn and hind paw tissues. (A-C) qPCR showing expression levels of Il1b (A), tnf (B) and Il10 (C) mRNAs in the left hind paws and the effects of DI. (D-E) DI inhibition of CFA-induced upregulation of Il1b (D) and tnf (E) in the L4–L5 spinal cord. *p < 0.05, **p < 0.01, ***p < 0.001 and ****p < 0.0001; n = 4 mice/group. (F) H&E staining showing the

inflammatory cell infiltration of paw tissues of 4 groups mice. Scale bar: 400 μm (top panels) and 100 μm (bottom panels), n = 3 mice/group.

Supplementary Files

This is a list of supplementary files associated with this preprint. Click to download.

- Additionalfile1.docx